Applied Catalysis B: Environmental 90 (2009) 99–104

Contents lists available at ScienceDirect

Applied Catalysis B: Environmental

journal homepage: www.elsevier.com/locate/apcatb

Methanol synthesis from sulfur-containing syngas over Pd/CeO_2 catalyst

Yuchun Ma [a,b], Qingjie Ge [a,*], Wenzhao Li [a], Hengyong Xu [a,1,*]

[a] Laboratory of Applied Catalysis, Dalian Institute of Chemical Physics, Chinese Academy of Sciences, Dalian 116023, China
[b] Graduate School of Chinese Academy of Sciences, Beijing 100039, China

ARTICLE INFO

Article history:
Received 1 November 2008
Received in revised form 12 February 2009
Accepted 25 February 2009
Available online 13 March 2009

Keywords:
Pd/CeO_2
Sulfur-tolerance
Methanol synthesis

ABSTRACT

Methanol synthesis from sulfur-containing syngas over Pd/CeO_2 catalyst has been investigated in this study, the characterization methods like X-ray powder diffraction (XRD), X-ray fluorescence (XRF), X-ray photoelectron spectroscopy (XPS) and pulse experiments has also been carried out for elucidating sulfur-tolerant mechanism of Pd/CeO_2 catalyst. The results show that methanol synthesis from sulfur-containing syngas exhibit stable reaction activity over Pd/CeO_2. It was indicated from characterization analysis that the sulfur-tolerance of Pd/CeO_2 was due to the capability of CeO_2 for transforming H_2S to SO_x. Thus, Pd active sites for methanol synthesis were protected from sulfur poisoning, which was the main deactivation reason of Pd/Al_2O_3 catalysts. A sulfur-tolerant model of Pd/CeO_2 catalyst for syngas to methanol was proposed according to the reaction performance and characterization results, which might be expanded to other sulfur-containing feed gas reaction systems over metal/ceria-type oxides.

1. Introduction

Methanol will play a major role in the energy sector, where it could provide a convenient hydrogen source for fuel cells, or serve as intermediate for synthetic fuels such as dimethyl ether (DME) [1–3]. As an important chemical intermediate and peak shaving fuel, methanol is the top-priority product of the integrated gasification combined cycle (IGCC) process, which could realize clean co-generation of electricity, chemicals and fuel gases from coal. Yet, IGCC syngas still contains at least 40 ppm sulfur if desulfurization by acid gas removal technologies, while conventional $Cu/ZnO/Al_2O_3$ catalysts for methanol synthesis do not tolerate more than 0.1 ppm H_2S due to the formation of metal sulfides [4]. Moreover, deep desulfurization of syngas will be impractical both from an environmental and economic point of view if methanol is produced as peak shaving fuel in the IGCC process. Therefore, studies on the sulfur-tolerant catalysts for methanol synthesis are becoming important and attractive to the IGCC process.

The literatures about sulfur-tolerant catalysts for methanol synthesis are very scarce [5–8], which mainly focus on metal sulfide catalysts, especially noble metal sulfide such as $Rh_{17}S_{15}$ and $Pd_{16}S_7$ [6–8]. Nevertheless, the activities of noble metal sulfide catalysts are lower in syngas with sulfur than those in syngas without sulfur. Koizumi et al. reported a stable alkali-promoted sulfided Pd/SiO_2 for methanol synthesis from sulfur-containing syngas and found that the reaction activity decreased to only one third of their initial activity in the absence of sulfur [8]. So, improvement of catalytic performance, especially catalytic stability of sulfur-tolerant catalysts for methanol synthesis is still the key issue of sulfur-containing syngas to methanol.

Ceria is known as an excellent oxygen transfer catalyst, which is extensively applied in three-way, automotive, emissions-control catalysts, due to its oxygen-storage capacity (OSC) derived from its redox properties [9–11]. Redox of Ce^{4+}/Ce^{3+} pair plays a key role when the exhaust in automobiles oscillates between oxidizing and reducing conditions. Ceria is also considered as a high-temperature sulfur sorbent because of the product Ce_2O_2S regeneration by the reaction of Ce_2O_2S and SO_2 at above 773 K, which yields elemental sulfur [12–13].

Ceria-supported Pd catalysts have been reported to be effective for hydrogenation of carbon monoxide and carbon dioxide to methanol [14–16]. In our previous results [17], Pd/CeO_2 also exhibits a more stable reaction activity for methanol synthesis from syngas containing sulfur than Pd/Al_2O_3. However, sulfur-tolerant mechanism of Pd/CeO_2 is still not clear. Therefore, in this study, the sulfur-tolerance of Pd/CeO_2 for methanol synthesis has been studied in detail. The results show that the metal palladium but not metal sulfides are active centers for the reaction of sulfur-containing syngas to methanol. Based on the combination of reaction performance and characterization analysis like X-ray powder diffraction (XRD), X-ray fluorescence (XRF), Temperature programmed reduction (TPR), X-ray photoelectron spectroscopy (XPS) and pulse experiments, a sulfur-tolerant mechanism model of Pd/CeO_2 catalyst was established, which could be applied to other metal-catalyzed reaction systems.

* Corresponding author. Fax: +86 411 84691570.
E-mail addresses: geqj@dicp.ac.cn (Q. Ge), xuhy@dicp.ac.cn (H. Xu).
[1] Fax: +86 411 84581234.

0926-3373/$ – see front matter © 2009 Elsevier B.V. All rights reserved.
doi:10.1016/j.apcatb.2009.02.020

2. Experimental

2.1. Catalyst preparation

Pd/CeO_2 with 15 wt.% Pd loading was prepared by a conventional coprecipitation method. An aqueous solution containing palladium chloride (Johnson Matthey, GR grade) and cerium nitrate (Shanghai Chemicals & Agents Corp., GR) were added simultaneously with an aqueous solution of sodium carbonate (Shenyang Federal Agents Corp., GR) to a beaker containing 20 ml water under constant stirring. The precipitation temperature and pH value were maintained at 328 K and 8–9, respectively. After filtering, drying at 393 K overnight, and calcination in air at 633 K (6 h), the catalyst was pelletized at 20 MPa, crushed, and sieved to obtain 20–40 mesh particles. Pd/Al_2O_3 (Pd 15 wt.%) catalyst and blank support CeO_2 were prepared by the same procedures. Catalysts after reaction in sulfur-containing syngas were designated as Pd/CeO_2(S), Pd/Al_2O_3(S) and CeO_2(S).

2.2. Catalyst characterization

XRD of the samples was measured on a Philips CM-1 (Cu Kα, $\gamma = 0.1543$ nm) powder X-ray diffractometer. Typically, the data were collected from 10° to 90° (2θ) as conventional wide-angle XRD patterns. The software X'Pert Highscore was used to perform microstructure analysis.

XRF data were acquired on a Philips Magix601 spectrometer (Rh target).

Temperature-programmed reduction (H_2-TPR) of catalysts was carried out in a stream of 5 vol.% H_2 balanced with Ar at a flow rate of 30 ml/min. After dehydration of a 50 mg sample at 523 K and cooling to room temperature under an Ar stream in a quartz tube, it was switched to 5% H_2/Ar and heated at a rate of 5 K/min. Formed water was trapped by dry ice with cooling ethanol. The hydrogen concentration in the effluent was continuously monitored by a thermal conductivity detector (Shimadzu, GC-8A).

XPS of the catalyst samples were recorded at room temperature using a Vacuum Generator Scientific ESCALAB Mark II system with Al-Kα ($h\upsilon = 1486.6$ eV, 10.0 kV) X-ray radiation. The power of the X-ray source was 100 W and the nominal resolution was higher than 0.1 eV. The background pressure in the analyzing chamber was kept below 7.5×10^{-8} Torr. Survey (0–1000 eV) and high-resolution spectra of Ce(3d), S(2p) and O(1s) were acquired, respectively. The C(1s) line at 284.6 eV was taken as a reference for binding energy (BE) calibration.

Pulse experiments were performed on a micro-pulse instrument with a conventional fixed-bed quartz reactor. 50 mg sample diluted by quartz sand was used for every test. Syngas for pulse composed of 31.7% CO, 63.3% H_2 and 5.0% N_2 was introduced into reactor by a six-way valve (0.3 ml). Pure hydrogen sulfide and air were taken into reactive system by injection (0.5 ml/pulse for H_2S and 2.0 ml/pulse for air). Before starting pulse experiments, catalyst was pre-reduced in 10% H_2/Ar at 723 K for 8 h. Pure syngas, hydrogen sulfide and air were pulsed into reactor following the sequence of Syngas(1) → H_2S(i) → Syngas(2) → H_2S(ii) → Syngas(3) → Air → Syngas(4). Argon was used as carrier gas (25 ml/min). Effluent gases were analyzed by an online gas chromatograph (Shimadzu, GC-8A) with a Porapak Q column and a TCD detector. Pulse experiments were carried out at 1.013×10^5 Pa and 723 K.

2.3. Catalytic activity test

A pressurized flow type reaction apparatus with a fixed-bed reactor was used for this study. The apparatus was equipped with a tubular reactor with an inner diameter of 8 mm, mass flow controllers for gas flows and a back-pressure regulator. The reaction temperature was controlled by a programmable temperature controller and detected by a thermocouple inside the catalyst bed.

Unless noted elsewhere, 0.4 g of catalyst was placed in the reactor with inert quartz sand above and under the catalyst. The catalyst was activated in a flow of 10% hydrogen in argon at 513 K for 8 h. The composition of feed-gas was 61.3% H_2, 30.6% CO, 5.1% CO_2, 3.0% N_2 (and 30 ppm H_2S (all volume)). Typically the reaction was carried at 513 K, 3.0 MPa and 1000 h^{-1}, respectively. A gas chromatograph (Shimadzu, GC-14B PTF), equipped with a carbon molecular sieve column and a porapak Q column, was used to analyze the products. N_2 was used as an internal standard for analysis.

3. Results and discussion

3.1. Catalytic activity of Pd/CeO_2 for methanol synthesis

Fig. 1 shows the catalytic behavior of Pd/CeO_2 catalyst for methanol synthesis from 30 ppm H_2S-containing syngas and sulfur-free syngas. An induction period existed at the initial stage of reaction over Pd/CeO_2 catalyst from syngas with the presence/absence of sulfur. Methanol selectivity increased in the induction period and then reached to stable. It's well accepted that Pd (1 1 1) plane adjacent to ceria is the efficient active sites for methanol formation, whereas the surface structure of Pd covered with thin layers of reduced ceria is important for methane formation. Naito et al. [18] investigated the effect of water pretreatment on methanol and methane formation active centers in CO–H_2 reaction using IR. They found that thin layers of reduced ceria covered on (1 1 1) plane of Pd particles could be removed by formed H_2O during reaction or H_2O pretreatment, which were responsible for the increment of methanol selectivity in the induction period. After induction period, the conversion of CO over Pd/CeO_2 catalyst came to stable and remained higher than 18% even after 100 h reaction in the presence of 30 ppm syngas. Methanol selectivity was stable after induction period and kept 89.1% after 100 h with the main by-products of methane and carbon dioxide. Compared with the activity in 30 ppm sulfur syngas, conversion of CO in sulfur-free syngas was only 2% higher after 100 h with an 83% CH_3OH selectivity. Notably that methanol selectivity over Pd/CeO_2 in sulfur-containing syngas was higher than that of in pure syngas, indicating that the surficial properties of catalyst had been modified in some extent which leads to a decrease of methane selectivity. The activities in sulfur-containing syngas in our study were basically equivalent to the results in pure syngas reported by

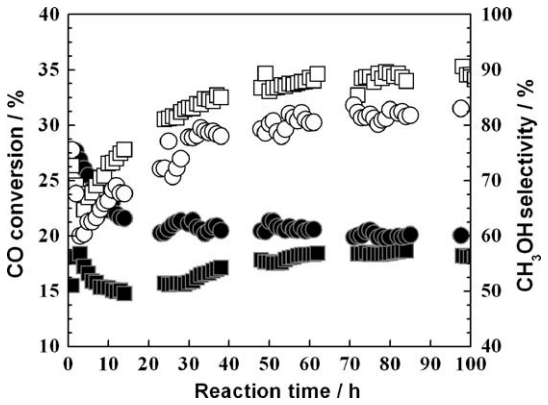

Fig. 1. CO conversion (full symbols) and CH_3OH selectivity (open symbols) over Pd/CeO_2 for methanol synthesis from syngas with 30 ppm H_2S (squares) or without H_2S (circles).

Matsumura et al. [15]. Considering that the active sites for methanol synthesis were palladium centers, a conclusion could be drawn that catalytic activity of Pd centers is well preserved on ceria in the presence of H_2S.

Fig. 2 reveals the yields of primary products in methanol synthesis from syngas with/without sulfur. Methanol yield in sulfur-containing syngas increased gradually in the induction period and was practically identical, i.e. 16.4%, in the absence of H_2S syngas, which indicates that the catalytically active Pd centers were rarely affected by H_2S. The CO_2 yield dropped with time and was noticeably lower after H_2S addition, i.e. 0.7% vs. 1.4% after 100 h, which indicates that CO oxidation slowed down in the sulfur-containing syngas. Furthermore, the catalytic sites for methane were distinct from those for methanol formation. Methane selectivity decreased quickly in the induction period which coincided with the transformation of methane sites well. Possibly their lower yields in sulfur-containing syngas was due to the blocking of methane active sites by sulfur.

It could be concluded that the Pd/CeO_2 catalyst was very active and stable in sulfur-containing syngas and exhibited excellent catalytic performance for sulfur-tolerant methanol synthesis. In order to further understand the sulfur-tolerant nature of Pd/CeO_2 catalyst for syngas to methanol, some characterization methods were carried out in the following sections.

3.2. X-ray diffraction (XRD) and X-ray fluorescence (XRF)

XRD and XRF techniques were used to make clear how the sulfur affected on the catalytic behavior of Pd/CeO_2 in reaction.

Fig. 3 compares the patterns of Pd/CeO_2 before/after 100 h reaction in sulfur-containing syngas. Only characteristic peaks of CeO_2 but no PdO were shown in the pattern of fresh catalyst before reduction, indicating that palladium oxide was highly dispersed on catalyst. After reduced at 513 K, Pd(1 1 1) peak was visible besides CeO_2 peaks. Ce_2O_3 peaks were not distinct due to the low reductive extent of CeO_2 at 513 K, which was a relative lower temperature for the reduction of CeO_2. Only Pd and ceria but neither PdS nor other sulfur compounds were detected by XRD on the sulfur-exposed $Pd/CeO_2(S)$ catalyst after the 100 h reaction. In contrast to the results over $Pd/CeO_2(S)$, PdS was found over $Pd/Al_2O_3(S)$ catalyst after 100 h reaction in sulfur-containing syngas.

XRF results of used catalysts were shown in Table 1. After 100 h reaction, XRF analysis revealed only 0.032 wt.% of sulfur corresponding to 6% of the total H_2S feed retained by Pd/CeO_2 catalyst. $Pd/Al_2O_3(S)$ catalyst after 100 h reaction in sulfur-containing syngas was tested for comparison. XRF results revealed the sulfur in feed gas was quantitatively adsorbed by Pd/Al_2O_3 catalyst. XRD

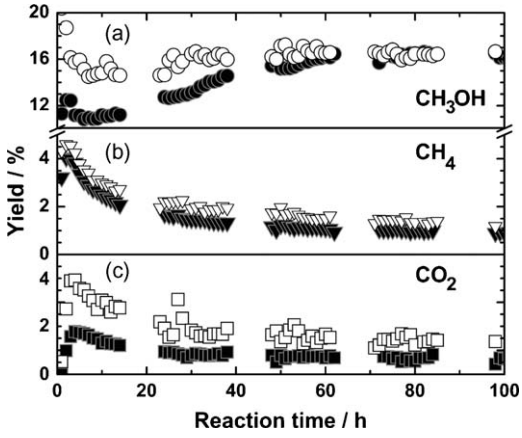

Fig. 2. (a) CH_3OH, (b) CH_4, and (c) CO_2 yield over Pd/CeO_2 from syngas containing no (open symbols) and 30 ppm H_2S (full symbols).

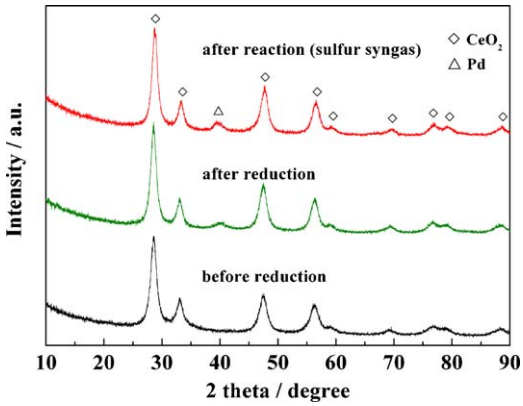

Fig. 3. XRD patterns of fresh Pd/CeO_2 and used $Pd/CeO_2(S)$ catalysts.

results showed the presence of PdS besides Pd and Al_2O_3 on $Pd/Al_2O_3(S)$ after 100 h operation in syngas with 30 ppm H_2S. Hence, combined with XRD and XRF results, the noble metal does not appear to be poisoned on Pd/CeO_2 catalyst.

3.3. Temperature-programmed reduction (H_2-TPR)

Fig. 4 displays the TPR profiles of fresh and used Pd/CeO_2 catalyst. The TPR profiles of the two samples were quite similar and both exhibit three main peaks. The first peak around 370.6 K was negative and could be assigned to the decomposition of PdH_2 [14,19]. Notably, the amount of given-off H_2 on Pd/CeO_2 catalyst, which was estimated by integrating the area of the curve, was very close to that on $Pd/CeO_2(S)$. That indicated the active Pd centers on the used catalyst were not affected by sulfur.

The consumption H_2 peak at medium temperature (ca. 673 K) by fresh catalyst was attributed to the reduction of the most easily reducible surface-capping oxygen of ceria according to literatures [14,20]. The last peak in TPR profiles could be assigned to the reduction of bulk CeO_2.

3.4. X-ray photoelectron spectroscopy (XPS)

Fig. 5 presents Ce(3d) XPS spectra of fresh samples (Pd/CeO_2, CeO_2) and used samples in sulfur-containing syngas ($Pd/CeO_2(S)$). There were two sets of spin-orbit multiplets: μ and υ correspond to $3d_{3/2}$ and $3d_{5/2}$ contributions of Ce(3d), respectively; the spectrum contained four main $3d_{5/2}$ features at ca. 881.3 (υ), 884.4 (υ1), 888.2 (υ2) and 897.6 (υ3) eV and four main $3d_{3/2}$ features at ca. 899.8 (μ), 903.9 (μ1), 906.6 (μ2) and 916.0 (μ3) eV. According to the assignment convention proposed by Burroughs et al. [21], the states of υ1 and μ1 belonged to unique photoelectron features from the Ce^{3+} state and the others could be attributed to Ce^{4+} [11,14,22–26]. The intensities of Ce^{3+}-related peaks in Fig. 5 decreased following the sequence $Pd/CeO_2(S)$>Pd/CeO_2>$CeO_2(S)$>CeO_2.

It could be concluded from Fig. 5 that, firstly, the amount of Ce^{3+} ions increased on the surface of catalysts after reaction in sulfur syngas, indicating that ceria was further reduced and lattice oxygen were partially consumed during exposure to sulfur

Table 1
The XRD and XRF results of used catalysts in sulfur-containing syngas.

Catalyst	Crystalline Phase (XRD)	S wt.% in Catalyst[a] (XRF)
$Pd/CeO_2(S)$	Pd, CeO_2	0.032 (0.520)
$Pd/Al_2O_3(S)$	Pd, Al_2O_3, PdS	0.520 (0.520)

[a] The numbers in bracket are the calculated amounts of sulfur in syngas streamed over catalysts in 100 h.

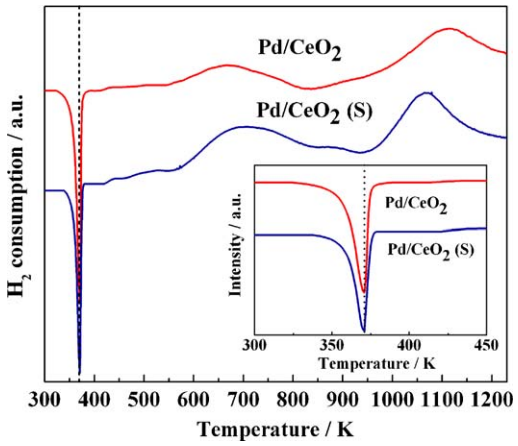

Fig. 4. H_2–TPR profiles of fresh Pd/CeO_2 and used $Pd/CeO_2(S)$ catalysts.

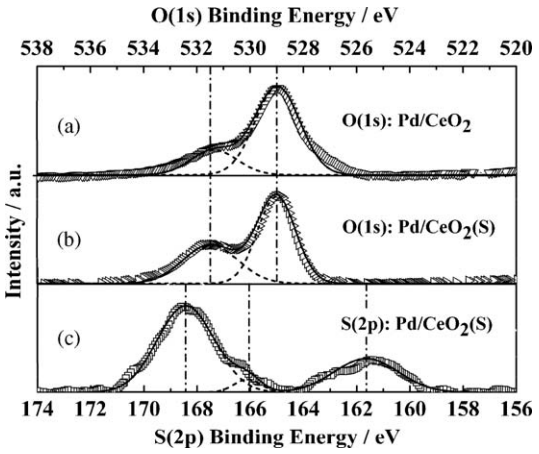

Fig. 6. (a), (b) O(1 s) XPS spectra of Pd/CeO_2 and $Pd/CeO_2(S)$ and (c) S(2p) XPS spectrum of $Pd/CeO_2(S)$.

atmosphere; secondly, the presence of Pd promoted the reduction of ceria. In order to clarify the effect of sulfur in feed gas on ceria valence, Ce(3d) XPS spectra need to be analyzed and quantified more accurately. However, it is an extraordinarily difficult problem due to the complex orbital hybridization of Ce(4f)/O(2p) and the overlapped of Ce^{3+} and Ce^{4+} peaks in Ce(3d) XPS. Fortunately, O(1s) photoelectron are sensitive to the electronic state of Ce and can be much more readily analyzed [27].

The O(1s) spectra of Pd/CeO_2 and $Pd/CeO_2(S)$ samples are presented in Fig. 6 (Fig. 6a, b). Two different oxygen bands can be discerned at 529.0 and 531.5 eV. The band in 529.0 eV can be assigned to oxygen bonded to two Ce^{IV} atoms and another one is oxygen linking a Ce^{IV} with a Ce^{III} atom [14,27–29]. The intensity of O(1 s) signal at 531.5 eV in Fig. 6b is much higher than that in Fig. 6a, implying the surface oxygen was consumed after reacted with sulfur and support ceria was further reduced. According to relative intensities the fresh catalyst contained already 20% Ce^{III} and this level rose to almost 25% in $Pd/CeO_2(S)$, which agrees well with Ce(3d) XPS spectra.

The S(2p) XPS of the sulfur traces on $Pd/CeO_2(S)$ exhibits two main peaks at 161.7 eV and 168.5 eV and a trivial peak at 166.0 eV (Fig. 6c). The weaker feature signal at 161.7 eV is sulfidic S^{2-} ions and peak at 166.0 eV is sulfur in + IV valence state (SO_2 or SO_3^{2-}), while the strongest one is characteristic for sulfur in the + VI oxidation state pointing to SO_3 (SO_4^{2-}) [30]. There is only very few sulfur retained by catalyst according to XRF data. The sulfur species appear to be well dispersed on Pd/CeO_2 catalyst since neither PdS nor sulfur compounds of Pd or Ce were detected by XRD.

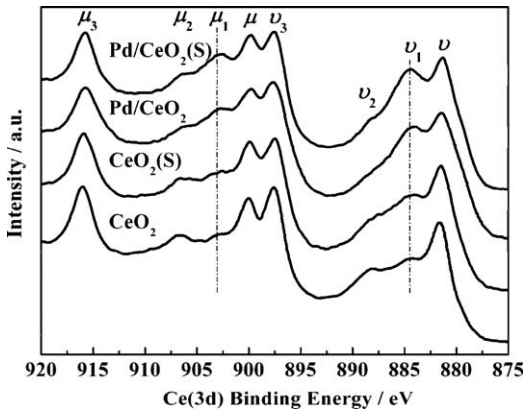

Fig. 5. Ce(3d) XPS spectra of fresh/used Pd/CeO_2 and ceria.

Considering that ceria is a sulfur sorbent in high temperature which reacts with sulfur to form Ce_2O_2S [12–13]. And based on thermodynamic model and reliable phase diagrams, it was reported that sulfur tends to react more readily with ceria under reducing conditions to form Ce_2O_2S than it does with precious metals to form corresponding sulfides [31]. It is consistent with our Pd(3d) XPS spectrum of $Pd/CeO_2(S)$ well, where the main Pd^0-related bands remained virtually unchanged, while only the very weak Pd^{II}-related bands shifted by 0.6–0.7 eV to lower energies with respect to those of pre-reduced fresh Pd/CeO_2. So the negligible amount of sulfur retained by catalyst is mainly oxidized to higher valence state by ceria according to S(2p) XPS.

From the XPS results of O(1s) and S(2p), the progressive reduction of support together with the evidence for S^{IV} and S^{VI} suggests that the following formal reaction occurs upon sulfur contact:

$$yH_2S + CeO_{2-x}\square_o \rightarrow CeO_{2-x-y}\square_o S_y + yH_2O, \quad (1a)$$

$$CeO_{2-x-y}\square_o S_y + CeO_{2-x}\square_o \rightarrow ySO_2 + 2CeO_{2-x-3/2y}\square_o, \quad (1b)$$

$$3ySO_2 + 2CeO_{2-x}\square_o \rightarrow 3ySO_3 + 2CeO_{2-x-3/2y}\square_o, \quad (1c)$$

$$CeO_{2-x-3/2y}\square_o + (1/2x + 3/4y)O_2 \rightarrow CeO_2. \quad (2)$$

Although it is likely that the SO_2 is prevailing in the reducing syngas atmosphere, SO_3 (SO_4^{2-}) is in domination from further oxidation of SO_2 (SO_3^{2-}) by S(2p) XPS results. Thus, the sulfur transformation on catalyst is as follows, H_2S reacted with ceria to form $CeO_{2-x-y}\square_o S_y$ firstly (Eq. (1a)) and then $CeO_{2-x-y}\square_o S_y$ undergone an oxidation process to SO_2 by ceria in the second step according to Eq. (1b), then progressive oxidation of SO_2 to SO_3 occurred upon reacting with ceria (Eq. (1c)). It must be pointed that the amount of sulfur (0.032 wt.%) is negligible compared with the amounts of H_2S (0.520 wt.%) streamed over catalyst in 100 h and cannot affect the activity of methanol synthesis. CeO_2 is consumed according to Eq. (1) and the sulfur-tolerance of Pd/CeO_2 catalyst may decline accordingly. In order to implement catalytic cycle the reduction of support needs to be reversed as shown in Eq. (2). This could be achieved by purging the reactor with an oxidant at intervals or more conveniently by adding a small amount of oxygen to the syngas mixture.

3.5. Pulse experiment

In order to elucidate the mechanism of sulfur transformation over Pd/CeO_2, pulse experiments were carried out at 723.15 K and

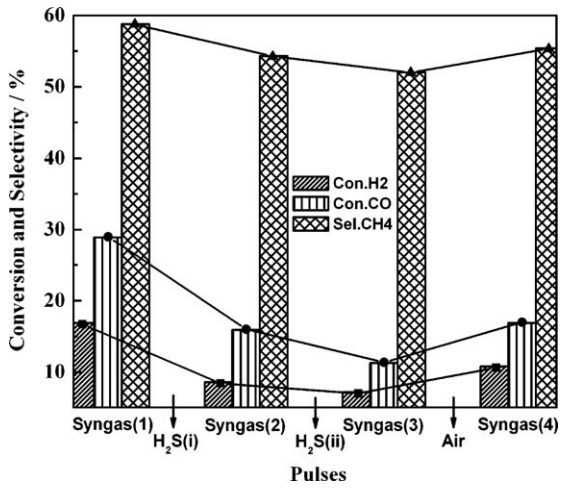

Fig. 7. CO and H_2 conversion and CH_4 selectivity in pulse experiments.

1.01×10^5 Pa. Methanation of CO hydrogenation was used as a probe reaction due to $CO + H_2$ at atmospheric pressure gives mainly rise to methane and trace methanol which cannot be detected by GC. Pure syngas, hydrogen sulfide and air were pulsed following the sequence: Syngas(1) → H_2S(i) → Syngas(2) → H_2S(ii) → Syngas(3) → Air → Syngas(4).

Fig. 7 reveals that CO conversion successively decreased after input of H_2S pulse. Conversion of CO is 28.9% in the first pulse and declined to 15.9% (Syngas(2)) and then to 11.3% (Syngas(3)) after two pulses of H_2S input. Note that a lot of SO_2 was detected from flow-out gases by GC after every H_2S pulse. This is another proof for sulfur transformation over Pd/CeO_2 catalyst and support S(2p) XPS data well. The remnant sulfur on catalyst may block and deteriorate the active sites for methanation in some content, which results in the continuous decline of methanation activity. This agrees well with the effect of sulfur on catalyst at 3.0 MPa (Fig. 2), in which the sulfur on catalyst causes a decrease of methane yield. After Syngas(3) pulse finished, air was injected into reactor. It's significative that CO conversion increased from 11.3% to 16.9% (Syngas(4)), indicating the poisoned catalytic centers for methanation recovered partly by oxidation treatment. The curves of H_2 conversion and CH_4 selectivity are similar to the trend of CO conversion. After air pulse injected, the selectivity of methane rises up from 52.1% to 55.4%.

Fig. 8 shows a compendious scheme of Pd/CeO_2 catalyst for methanation in the presence of sulfur. It could be concluded that H_2S reacts firstly with ceria and deteriorates the active centers of methanation. Oxygen in air recovers the active sites for methanation mostly. The sulfur retained by catalyst is oxidized to SO_2 by ceria over Pd/CeO_2.

Based on the XPS, XRD and pulse experiments results, a new sulfur-tolerant model for methanol synthesis over Pd/CeO_2 catalyst was established and shown in Fig. 9. Pd/CeO_2 realizes a bifunctional catalytic property in this model, in which methanol synthesis occurred mainly on Pd active sites and sulfur transformed on support ceria. H_2S reacts with $Pd/CeO_{2-x}\square_o$ to form $Pd/CeO_{2-\delta}\square_oS_y$ species firstly, whereafter the sulfur over $Pd/CeO_{2-\delta}\square_oS_y$ is oxidized to SO_2, and then a progressive oxidation of SO_2 to SO_3 occurs over catalyst lastly. A slightly amount O_2 that existed in feedstock or purged into reactor at intervals for purpose of activating catalyst can reoxidize support to CeO_2.

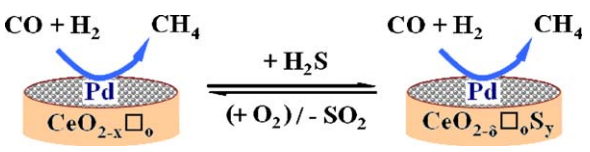

Fig. 8. A compendious scheme of Pd/CeO_2 ($x < \delta < 0.5$) catalyst for methanation in the presence of sulfur.

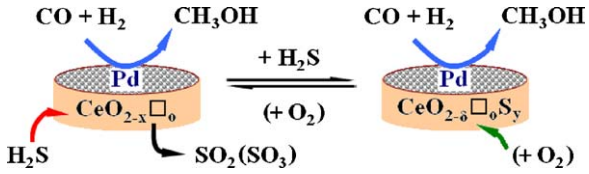

Fig. 9. Scheme of bifunctional Pd/CeO_2 ($x < \delta < 0.5$) catalyst model for methanol synthesis in the presence of sulfur.

Altogether, accompanied with methanol synthesis process, the sulfur in feed gas is oxidized and undesired side reactions leading to methane, CO_2 and hydrocarbons are suppressed. Considering the role of CeO_2 and active metal in the catalyst, the above reaction model might be expanded to other sulfur-tolerant reaction systems over metal/ceria-type oxides catalysts, like Fisher–Tropsch synthesis, hydrogen-oxygen reaction etc, in which active metal could catalyze the reaction and support oxides could convert hydrogen sulfide.

4. Conclusions

The unique property of ceria protects the catalytic activity of active metal Pd for methanol synthesis from poisoning in sulfur-containing syngas at moderate reaction temperatures. A bifunctional sulfur-tolerant model of Pd/CeO_2 catalyst for methanol synthesis had been established. In the process of methanol synthesis from sulfur-containing syngas, H_2S transformation mainly occurs on support ceria and reacts with ceria instead of the active Pd metal to form sulfur oxide, and CO hydrogenation to form methanol mainly occurs on active Pd centers. The active Pd centers are preserved from sulfur poisoning and a high activity of the catalyst is achieved, which is responsible for the high stability of methanol synthesis on Pd/CeO_2. Methanol synthesis from sulfur-containing (30 ppm H_2S) syngas exhibits stable reaction activity over Pd/CeO_2: 18% CO conversion and 90% methanol selectivity could be kept during 100 h reaction at 513 K, 3.0 MPa and 1000 h^{-1}.

Acknowledgements

This work was supported by BP through the clean energy facing the future program (CEFTF) at Dalian Institute of Chemical Physics, Chinese Academy of Sciences.

Appendix A. Supplementary data

Supplementary data associated with this article can be found, in the online version, at doi:10.1016/j.apcatb.2009.02.020.

References

[1] D. Mahajan, A.N. Goland, Catal. Today 84 (2003) 71.
[2] K.-A. Adamson, P. Pearson, J. Power Sources 86 (2000) 548.
[3] T.A. Semelsberger, R.L. Borup, H.L. Greene, J. Power Sources 156 (2006) 497.
[4] M.V. Twigg, M.S. Spencer, Top. Catal. 22 (2003) 191.
[5] M.N. Berube, B. Sung, M.A. Vannice, Appl. Catal. 31 (1987) 133.
[6] M. Yamada, N. Koizumi, A. Miyazawa, T. Furukawa, Catal. Lett. 78 (2002) 195.
[7] N. Koizumi, A. Miyazawa, T. Furukawa, M. Yamada, Chem. Lett. 30 (2001) 1282.
[8] N. Koizumi, K. Murai, S. Tamayama, T. Ozaki, M. Yamada, Energ. Fuel 17 (2003) 829.
[9] H.C. Yao, Y.F.Y. Yao, J. Catal. 86 (1984) 254.
[10] A. Morikawa, T. Suzuki, T. Kanazawa, K. Kikuta, A. Suda, H. Shinjo, Appl. Catal. B 78 (2008) 210.

[11] Z. Chen, Q. Gao, Appl. Catal. B 84 (2008) 790.
[12] Y. Zeng, S. Zhang, F.R. Groves, D.P. Harrison, Chem. Eng. Sci. 54 (1999) 3007.
[13] M. Flytzani-Stephanopoulos, M. Sakbodin, Z. Wang, Science 312 (2006) 1508.
[14] W.J. Shen, Y. Ichihashi, H. Ando, Y. Matsumura, M. Okumura, M. Haruta, Appl. Catal. A 217 (2001) 231.
[15] Y. Matsumura, W.J. Shen, Y. Ichihashi, M. Okumura, J. Catal. 197 (2001) 267.
[16] C. Sudhakar, M.A. Vannice, J. Catal. 95 (1985) 227.
[17] Y. Ma, Q. Ge, W. Li, H. Xu, Catal. Commun. 10 (2008) 6.
[18] S. Naito, T. Kasahara, T. Miyao, Catal. Today 74 (2002) 201.
[19] M.L. Cubeiro, J.L.G. Fierro, Appl. Catal. A 168 (1998) 307.
[20] C. de Leitenburg, A. Trovarelli, J. Kašpar, J. Catal. 166 (1997) 98.
[21] P. Burroughs, A. Hamnett, A.F. Orchard, G. Thornton, J. Chem. Soc., Dalton Trans. (1976) 1686.
[22] H. He, H.X. Dai, C.T. Au, Catal. Today 90 (2004) 245.
[23] F. Giordano, A. Trovarelli, C. de Leitenburg, M. Giona, J. Catal. 193 (2000) 273.
[24] J.Z. Shyu, K. Otto, W.L. Watkins, G.W. Graham, R.K. Belitz, H.S. Gandhi, J. Catal. 114 (1988) 23.
[25] F. Le Normand, L. Hilaire, K. Kili, G. Krill, G. Maire, J. Phys. Chem. 92 (1988) 2561.
[26] J. Liu, Z. Zhao, J. Wang, C. Xu, A. Duan, G. Jiang, Q. Yang, Appl. Catal. B 84 (2008) 185.
[27] Y. Matsumura, W.J. Shen, Y. Ichihashi, Y. Morisawa, M. Okumura, Chem. Lett. 29 (2000) 880.
[28] A. Trovarelli, G. Dolcetti, C. de Leitenburg, J. Kašpar, P. Finetti, A. Santoni, J. Chem. Soc., Faraday Trans. 88 (1992) 1311.
[29] A. Laachir, V. Perrichon, A. Badri, J. Lamotte, E. Catherine, J.C. Lavalley, J. El Fallah, L. Hilaire, F. Le Normand, E. Quéméré, G.N. Sauvion, O. Touret, J. Chem. Soc., Faraday Trans. 87 (1991) 1601.
[30] M.-D. Appay, J.-M. Manoli, C. Potvin, M. Muhler, U. Wild, O. Pozdnyakova, Z. Paál, J. Catal. 222 (2004) 419.
[31] H. Karljalainen, U. Lassi, K. Rahkamaa-Tolonen, V. Kröger, R.L. Keiski, Catal. Today 100 (2005) 291.